

Renormalized behavior and proximity to a magnetic quantum critical point in BaCo_2As_2

A.S. Sefat, D.J. Singh, R. Jin, M.A. McGuire, B.C. Sales, D. Mandrus

Materials Science and Technology Division, Oak Ridge National Laboratory, Oak Ridge, Tennessee 37831-6114

(Dated: October 30, 2018)

We report synthesis and single crystal measurements of magnetic, transport and thermal properties of single crystalline BaCo_2As_2 as well as first principles calculations of the electronic structure and magnetic behavior. These results show that BaCo_2As_2 is a highly renormalized paramagnet in proximity to a quantum critical point, presumably of ferromagnetic character and that BaFeNiAs_2 behaves similarly. These results are discussed in relation to the properties of $\text{Ba}(\text{Fe},\text{Co})_2\text{As}_2$ and $\text{Ba}(\text{Fe},\text{Ni})_2\text{As}_2$, which are superconducting for low Co and Ni concentrations.

PACS numbers: 71.20.Lp, 65.40.Ba, 75.10.Lp

The discovery of high temperature superconductivity in oxy-pnictide phases, prototype $\text{LaFeAs}(\text{O},\text{F})$ by Kamihara and co-workers¹ has led to strong interest in establishing the physical properties of these materials and the mechanism of superconductivity. Since the discovery, superconductivity has been found in a rather wide variety of compounds with Fe^{2+} square planar sheets. These include the oxy-pnictides, doped ThCr_2Si_2 structure compounds of e.g. BaFe_2As_2 ,² LiFeAs ,³ and FeSe .⁴ Remarkably, superconductivity can be produced in BaFe_2As_2 by alloying Fe with the other ferromagnetic $3d$ elements, Co or Ni,^{5,15} as is also found in the oxy-pnictides.⁷ Interestingly, both the Ni-based oxy-pnictide and BaNi_2As_2 are superconductors,^{8,9,10} although the critical temperatures are much lower than in the Fe-based compounds and the mechanism may be different.^{11,12} Also, LaCoAsO and LaCoPO are itinerant ferromagnets.^{7,13}

The single crystals of BaCo_2As_2 were grown out of CoAs flux. The typical crystal sizes were $\sim 5 \times 3 \times 0.2$ mm. High purity elements ($> 99.9\%$, from Alfa Aesar) were used in the preparation of the crystals. First, CoAs binary was prepared by placing mixtures of arsenic pieces, and cobalt powder in a silica tube. These were reacted slowly by heating to 300°C (dwell 10 hrs), to 600°C (dwell 10 hrs), then to 900°C (dwell 10 hrs). Then, a ratio of Ba:CoAs = 1:5 was heated in an alumina crucible for 15 hours at 1180°C under a partial atmosphere of argon. This reaction was cooled at the rate of $2^\circ\text{C}/\text{hour}$, followed by decanting of CoAs flux at 1090°C . The crystals were well-formed plates with the $[001]$ direction perpendicular to the plane. Electron probe microanalysis of a cleaved surface of the single crystal was performed on a JEOL JSM-840 scanning electron microscope using an accelerating voltage of 15 kV and a current of 20 nA with an EDAX brand energy-dispersive X-ray spectroscopy (EDS) device. EDS analyses indicated Ba:Co:As ratio of 1:2:2. The structural identification was made via powder x-ray diffraction, using a Scintag XDS 2000 $\Theta - \Theta$ diffractometer (Cu K_α radiation). The cell parameters were refined using least squares fitting of the measured peak positions in the range 2Θ from $10 - 90^\circ$ using the Jade 6.1 MDI package. The lattice parameters of BaCo_2As_2 are $a = 3.954(1)$ Å, and $c = 12.659(3)$ Å,

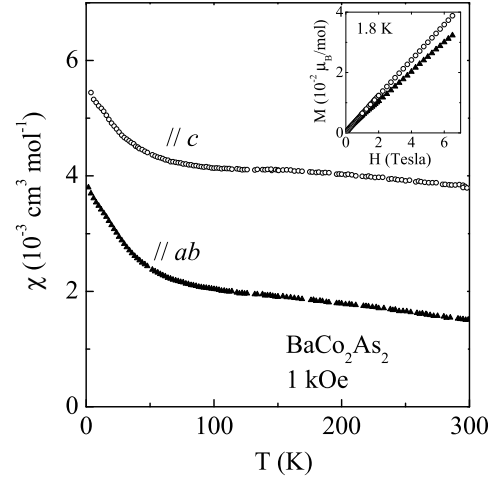


FIG. 1: Magnetic measurements for BaCo_2As_2 along the two crystallographic directions. The figure is the temperature dependence of the zero-field cooled magnetization in 1 kOe; inset is the field dependence of the magnetization at 1.8 K.

in the ThCr_2Si_2 structure ($I4/mmm$, $Z = 2$) in close agreement with the report of Ref. 14.

DC magnetization was measured as a function of temperature and field using a Quantum Design Magnetic Property Measurement System. Fig. 1 shows the susceptibility in 1 kOe applied field along c - and ab -crystallographic directions. The susceptibility is weakly anisotropic and decreases with increasing temperature. At 1.8 K, $\chi_c = 5.4 \times 10^{-3} \text{ cm}^3 \text{ mol}^{-1}$ and $\chi_{ab} = 3.8 \times 10^{-3} \text{ cm}^3 \text{ mol}^{-1}$. As seen in the inset of Fig. 1 the field dependent magnetization is linear at 1.8 K.

Temperature dependent electrical resistivity measurements were performed on a Quantum Design Physical Property Measurement System (PPMS), measured in both the ab plane (ρ_{ab}) and c direction (ρ_c). As shown in Fig. 2, both ρ_{ab} and ρ_c decrease with decreasing temperature, revealing metallic behavior. However, the resistivity is much more anisotropic than the magnetic sus-

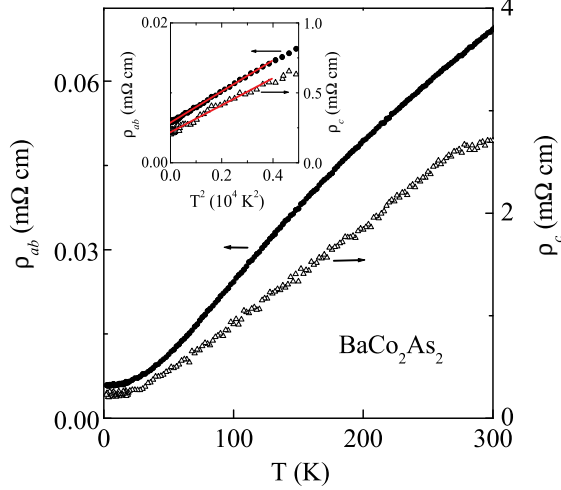


FIG. 2: Temperature dependence of the resistivity of BaCo_2As_2 in zero field for the two crystallographic directions.

ceptibility. At room temperature $\rho_{ab} = 0.07 \text{ m}\Omega \text{ cm}$ and $\rho_c = 2.7 \text{ m}\Omega \text{ cm}$, resulting in $\rho_c/\rho_{ab} \sim 39$. In analyzing the low temperature data, we found that both ρ_{ab} and ρ_c exhibit quadratic temperature dependences in a wide temperature range. Shown in the inset of Fig. 2 is the plot of $\rho_{ab}(T^2)$ and $\rho_c(T^2)$ between 1.8 and 71 K. Note that ρ_{ab} and ρ_c vary approximately linearly with T^2 below $\sim 60 \text{ K}$. By fitting the resistivity data between 1.8 and 60 K using $\rho_{ab,c} = \rho_{ab,c}(0 \text{ K}) + AT^2$, we obtain the residual resistivity $\rho_{ab}(0 \text{ K}) = 5.75 \text{ }\mu\Omega \text{ cm}$, $\rho_c(0 \text{ K}) = 0.22 \text{ m}\Omega \text{ cm}$, and constant $A_{ab} = 2.22 \times 10^{-3} \text{ }\mu\Omega \text{ cm/K}^2$, $A_c = 9.65 \times 10^{-2} \text{ }\mu\Omega \text{ cm/K}^2$. These give the residual-resistivity-ratio ($\rho_{300\text{K}}/\rho_{0\text{K}}$) ~ 12 along both crystallographic directions, indicating good crystal quality. The quadratic temperature dependence of the electrical resistivity reflects the importance of the Umklapp process of the electron-electron scattering at low temperatures and is consistent with the formation of a Fermi-liquid state. Interestingly, the system shows little magnetoresistance under application is magnetic field up to 8 Tesla.

Specific heat data, $C_p(T)$, were also obtained using the PPMS via the relaxation method. Fig. 3 gives the temperature dependence of specific heat. Below $\sim 7 \text{ K}$, C/T vs. T^2 is linear (inset of Fig. 3) consistent with a Fermi liquid plus phonon contribution. In the temperature range of 1.9 K to $\sim 7 \text{ K}$, the fitted Sommerfeld coefficient, γ , is $8.2 \text{ mJ}/(\text{K}^2 \text{ mol atom})$ or $20.5 \text{ mJ}/(\text{K}^2 \text{ mol Co})$. This is a high value that would correspond to an electronic density of states of 8.7 eV^{-1} per Co both spins. The mean field Stoner criterion ($NI > 1$, $I \sim 0.8 \text{ eV}$ per spin for $3d$ elements) for ferromagnetism would be strongly exceeded if this is interpreted as the bare electronic density of states for Co. The absence of magnetism therefore implies either strong hybridization with ligands, which is not evident in the electronic structure,

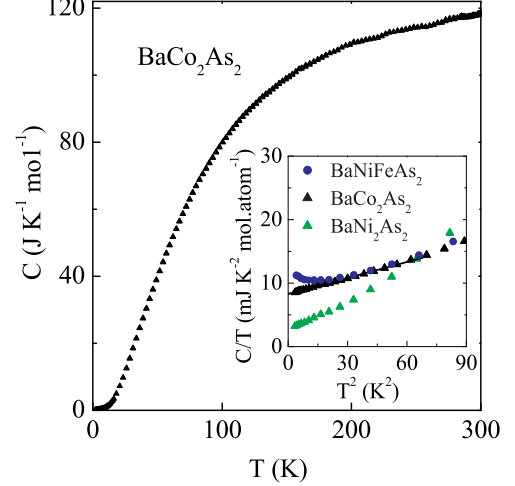


FIG. 3: (Color online) Temperature dependence of the specific heat of BaCo_2As_2 . The inset is C/T vs. T^2 and a linear fit to the data below $\sim 7 \text{ K}$ compared with data for BaFeNiAs_2 and BaNi_2As_2 .

or substantial renormalization due to e.g. spin fluctuations. Assuming that $\chi_c = 5.4 \times 10^{-3} \text{ mol}^{-1}$ and $\chi_{ab} = 3.8 \times 10^{-3} \text{ mol}^{-1}$ at 1.8 K are spin susceptibilities (i.e. assuming that the diamagnetic and van Vleck contributions are small), we may estimate the Wilson ratio $R_W = \pi^2 k_B^2 \chi_{spin} / (3\mu_B^2 \gamma)$. This gives $R_W \sim 7$ from χ_{ab} and ~ 10 from χ_c . These values well exceed unity for a free electron system and are indicative of enhanced magnetic behavior. There are several possible reasons for high R_W : one is that actual low-temperature spin susceptibility is much smaller than the total susceptibility e.g. due to a strong orbital contribution. Another source of enhancement can be strong Coulomb correlations, which often result in Wilson ratios intermediate between 1.5 and 2.0. However, the large value that we find, which is an order of magnitude higher, is best explained as indicating that the system is close to ferromagnetism. Combined with the high R_W , we find a normal Kadowaki-Woods ratio A/γ^2 . In particular, for BaCo_2As_2 in-plane transport we obtain $A_{ab}/\gamma^2 = 0.5 \times 10^{-5} \text{ }\mu\Omega \text{ cm}/(\text{mJ/mol-K})^2$. This is comparable to but larger than the value for the nearly two dimensional Fermi liquid, Sr_2RuO_4 , somewhat smaller than the typical value of $10^{-5} \text{ }\mu\Omega \text{ cm}/(\text{mJ/mol-K})^2$ for heavy Fermions, and significantly smaller than the values found in correlated oxides with frustration or other very strong scattering such as LiV_2O_4 or $\text{La}_{1.7}\text{Sr}_{0.3}\text{CuO}_4$.¹⁵

Electronic structure calculations were performed using the general potential linearized augmented planewave (LAPW) method with local orbitals,^{16,17} similar to those reported previously for BaFe_2As_2 .¹⁸ The calculations used LAPW sphere radii of 2.2, 2.1 and $2.1 a_0$ for Ba, Co and As, respectively, and were done within the local den-

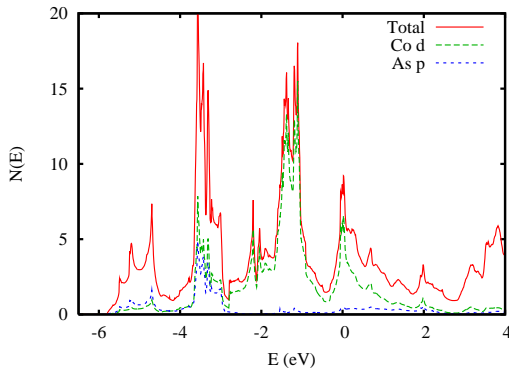


FIG. 4: LDA non-spin-polarized electronic density of states of BaCo_2As_2 on a per formula unit basis. The projections shown are onto the LAPW spheres.

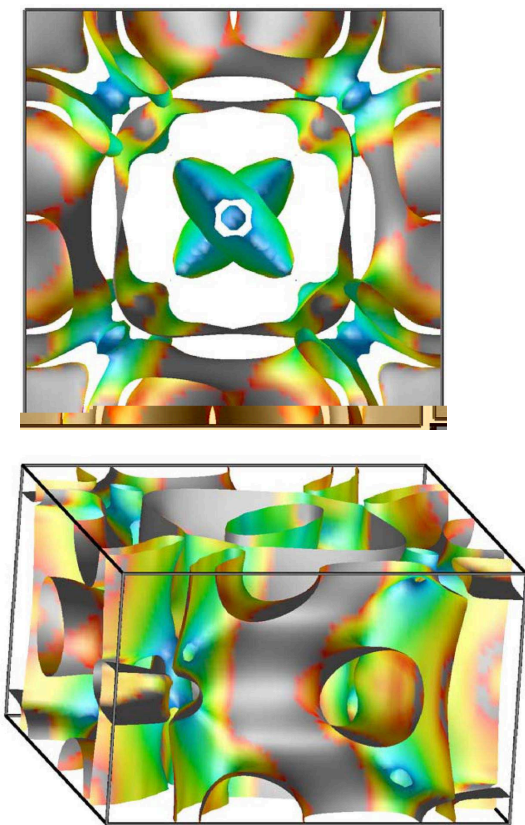


FIG. 5: (Color online) LDA non-spin-polarized Fermi surface of BaCo_2As_2 shaded by velocity; blue is low velocity. The corners are Γ and M (0,0,1/2) points in the body centered tetragonal zone.

sity approximation (LDA) with reported lattice parameters of $a=3.958 \text{ \AA}$, and $c=12.67 \text{ \AA}$.¹⁴ The As internal coordinate z_{As} was obtained by energy minimization as $z_{\text{As}}=0.34528$. The calculated electronic density of states (DOS) and Fermi surface are shown in Figs. 4 and 5.

The DOS is rather similar to that of the Fe compounds with the exception of the position of the Fermi energy. In

particular, it shows only modest covalency between Co and As, and has a pseudogap at an electron count of six d electrons per Co. The extra d electron in Co^{2+} relative to Fe^{2+} shifts E_F upwards into a region of high DOS. The Fermi surface is large and multi-sheeted, as shown in Fig. 5. The calculated Fermi surface has both two and three dimensional sheets, and in particular is more three dimensional than might be expected based on the anisotropy of the measured resistivity. Reconciling the Fermi surface with the transport data would require scattering that depends on the particular Fermi surface sheet, as may occur, for example, from spin fluctuations with a large anisotropy or due to strong band dependence of the electron phonon scattering. The main As contributions to the DOS are between -6 eV and -3 eV relative to E_F , corresponding to stable As^{3-} and Co^{2+} . The value at the Fermi energy is $N(E_F) = 8.5 \text{ eV}^{-1}$ on a per formula unit (two Co atoms) both spins basis. Comparing with the measured specific heat implies a mass renormalization of ~ 2 , similar to the Fe-based superconductors. As shown in the inset of Fig. 3, our measured value for BaNi_2As_2 is $\gamma = 15 \text{ mJ}/(\text{mol K}^2)$, as compared with a bare value from $N(E_F)$ of $8.9 \text{ mJ}/(\text{mol K}^2)$. This yields an enhancement factor of $(1 + \lambda) = 1.7$, consistent with the value of the electron-phonon $\lambda = 0.76$ obtained from first principles calculations for that compound.¹²

The physics, however, appears different in BaCo_2As_2 . First of all, the susceptibility implied by the magnetization measurements is enhanced over the Pauli susceptibility from the LDA density of states, $\chi_0 = 2.75 \times 10^{-4} \text{ emu/mol}$ by a factor of ~ 15 (depending on direction) yielding a high Wilson ratio with implied nearness to ferromagnetism. Furthermore, the non-renormalized LDA $N(E_F)$ is already large enough to lead to a mean field Stoner instability towards ferromagnetism. In fact, contrary to experiment we find a stable ferromagnetic ground state in the LDA, with spin moment $0.94 \mu_B$ per formula unit ($0.42 \mu_B/\text{Co}$) and energy 32 meV per formula unit lower than the non-spin-polarized solution. The total energy as a function of constrained moment is shown in Fig. 6. We also searched for an antiferromagnetic solution with a checkerboard in plane arrangement where all nearest neighbor Fe bonds are antiferromagnetic. However, we did not find a stable antiferromagnetic state of this type. This indicates that the stability of Fe moments depends on the particular magnetic order and therefore that the magnetism is itinerant. Thus at the LDA level, BaCo_2As_2 is a weak itinerant magnet, apparently ferromagnetic in-plane, though the out-of-plane interaction may be ferromagnetic or antiferromagnetic.

While the mechanism for superconductivity of the layered Fe compounds remains to be established, there is accumulating evidence of a relationship between superconductivity and magnetism. For example, the phase diagrams show an interplay between of an itinerant spin density wave with superconductivity,^{19,20} and density functional calculations show a proximity to magnetism, with evidence for strong spin fluctuations.^{21,22,23,24} Other

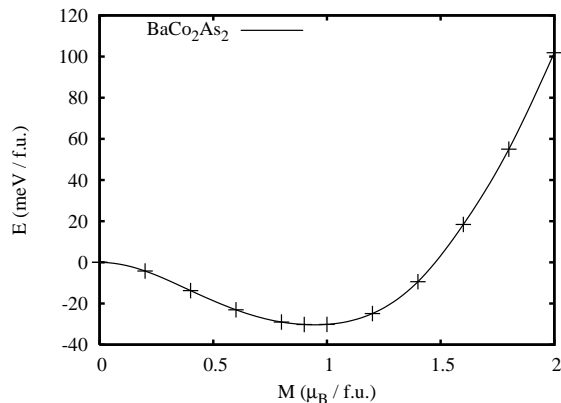


FIG. 6: LDA fixed spin moment energy as a function of constrained moment for BaCo_2As_2 .

evidence for strong magnetic effects comes from the unusual temperature dependence of the susceptibility, $\chi(T)$, which for some compounds is increasing with T up to high T ,^{25,26} and unusually large discrepancies between calculated and measured pnictogen crystallographic positions.²⁴ An important signature of the beyond mean field spin fluctuation effects in the Fe-based superconductors is the fact that standard density functional calculations give much more robust magnetic moments than experiment.

Comparing our experimental and calculated results for BaCo_2As_2 , we find a related situation. In particular, we do not find clear evidence in transport or magnetization data for a magnetic ordering (there is a change of behavior of the magnetization at ~ 60 K but the susceptibility continues increasing below this temperature, and we do not find any hysteresis). The implication is that the LDA yields a more magnetic state than experiment. This generally occurs in materials near a magnetic quantum critical point, where ordering is suppressed by quantum fluctuations in the order parameter (i.e. spin fluctuations). Examples of this behavior include the weak itinerant

ferromagnets ZrZn_2 , Ni_3Al and the highly renormalized paramagnets Ni_3Ga and $\text{Sr}_3\text{Ru}_2\text{O}_7$,^{27,28,29,30,31} although the renormalizations in those materials are apparently stronger than in our measurements for BaCo_2As_2 .

Further information comes from our single crystal measurements for BaFeNiAs_2 , which was prepared in a similar way to BaCo_2As_2 , using a near equal atomic mixture of Fe and Ni to obtain approximately the same average d electron count as BaCo_2As_2 . The single crystals of BaFeNiAs_2 were grown similar to that described above for BaCo_2As_2 . The measured specific heat γ (Fig. 3 is remarkably similar to those for BaCo_2As_2 . Therefore, at least for these properties, which include the renormalization, the material behaves as a virtual crystal, meaning that the alloy of Fe and Ni behaves in many respects as if it were a true pure compound of the element with the average atomic number (i.e. Co for an equal mixture). In this way, scattering is not strong enough to alter the basic electronic structure, a fact that may be of importance in understanding why superconductivity in the BaFe_2As_2 is robust against the disorder introduced by alloying with Co or Ni.

To summarize we find from comparison of experimental data on single crystals and LDA calculations that BaCo_2As_2 is a substantially renormalized metal near a magnetic quantum critical point, probably of ferromagnetic character. It will be of interest to tune the proximity to the critical point. One interesting possibility would be to alloy on the Ba-site with a magnetic element, e.g. Eu, which may favor formation of a magnetically ordered state.

Acknowledgments

Work was supported by the Department of Energy, Division of Materials Sciences and Engineering, Office of Basic Energy Sciences, U. S. Department of Energy.

- ¹ Y. Kamihara, T. Watanabe, M. Hirano, and H. Hosono, *J. Am. Chem. Soc.* **130**, 3296 (2008).
- ² M. Rotter, M. Tegel, and D. Johrendt, *Phys. Rev. Lett.* **101**, 107006 (2008).
- ³ X.C. Wang, Q.Q. Liu, Y.X. Lv, W.B. Gao, L.X. Yang, R.C. Yu, F.Y. Li, and C.Q. Jin, arXiv:0806.4688 (2008).
- ⁴ F.C. Hsu, J.Y. Luo, K.W. Yeh, T.K. Chen, T.W. Huang, P.M. Wu, Y.C. Lee, Y.L. Huang, Y.Y. Chu, D.C. Yan, and M.K. Wu, *Proc. Nat. Acad. Sci. (USA)* **105**, 14262 (2008).
- ⁵ A.S. Sefat, R. Jin, M.A. McGuire, B.C. Sales, D.J. Singh, and D. Mandrus, *Phys. Rev. Lett.* **101**, 117004 (2008).
- ¹⁵ L.J. Li, Q.B. Wang, Y.K. Luo, H. Chen, Q. Tao, Y.K. Li, X. Lin, M. He, Z.W. Zhu, G.H. Cao, and Z.A. Xu, arXiv:0809.2009 (2008).
- ⁷ A.S. Sefat, A. Huq, M.A. McGuire, R. Jin, B.C. Sales, and D. Mandrus, *Phys. Rev. B* **78**, 104505 (2008).

- ⁸ F. Ronning, N. Kurita, E.D. Bauer, B.L. Scott, T. Park, T. Klimczuk, R. Movshovich, and J.D. Thompson, *J. Phys. Condens. Matter* **20**, 342203 (2008).
- ⁹ T. Watanabe, H. Yanagi, Y. Kamihara, T. Kamiya, M. Hirano, and H. Hosono, *J. Solid State Chem.* **181**, 2117 (2008).
- ¹⁰ Z. Li, G.F. Chen, J. Dong, G. Li, W.Z. Hu, D. Wu, S.K. Su, P. Zheng, T. Xiang, N.L. Wang, and J.L. Luo, *Phys. Rev. B* **78**, 060504(R) (2008).
- ¹¹ A. Subedi, D.J. Singh, and M.H. Du, *Phys. Rev. B* **78**, 060506(R) (2008).
- ¹² A. Subedi and D.J. Singh, *Phys. Rev. B* **78**, 132511 (2008).
- ¹³ H. Yanagi, R. Kawamura, T. Kamiya, Y. Kamihara, M. Hirano, T. Nakamura, H. Osawa, and H. Hosono, *Phys. Rev. B* **77**, 224431 (2008).
- ¹⁴ M. Pfisterer and G. Nagorsen, *Z. Nat. B* **35**, 703 (1980).

- ¹⁵ S.Y. Li, L. Taillefer, D.G. Hawthorn, M.A. Tanatar, J. Paglione, M. Sutherland, R.W. Hill, C.H. Wang, and X.H. Chen, Phys. Rev. Lett. **93**, 056401 (2004).
- ¹⁶ D.J. Singh and L. Nordstrom, *Planewaves, Pseudopotentials and the LAPW Method, 2nd. Ed.* (Springer, Berlin, 2006).
- ¹⁷ D. Singh, Phys. Rev. B **43**, 6388 (1991).
- ¹⁸ D.J. Singh, Phys. Rev. B **78**, 094511 (2008).
- ¹⁹ C. de la Cruz, Q. Huang, J.W. Lynn, J. Li, W. Ratcliff II, J.L. Zarestsky, H.A. Mook, G.F. Chen, J.L. Luo, N.L. Wang, and P. Dai, arXiv:0804.0795 (2008).
- ²⁰ M. Rotter, M. Tegel, D. Johrendt, I. Schellenberg, W. Hermes, and R. Pottgen, Phys. Rev. B **78**, 020503(R) (2008).
- ²¹ D.J. Singh and M.H. Du, Phys. Rev. Lett. **100**, 237003 (2008).
- ²² I.I. Mazin, D.J. Singh, M.D. Johannes, and M.H. Du, Phys. Rev. Lett. **101**, 057003 (2008).
- ²³ Z.P. Yin, S. Lebegue, M.J. Han, S.Y. Savrasov, and W.E. Pickett, Phys. Rev. Lett. **101**, 047001 (2008).
- ²⁴ I.I. Mazin, M.D. Johannes, L. Boeri, K. Koepernik, and D.J. Singh, Phys. Rev. B **78**, 085104 (2008).
- ²⁵ H.-H. Klauss, H. Luetkens, R. Klingeler, C. Hess, F.J. Litterst, M. Kraken, M.M. Korshunov, I. Eremin, S.-L. Drechsler, R. Khasanov, A. Amato, J. Hamann-Borrero, N. Leps, A. Kondrat, G. Behr, J. Werner, and B. Buchner, Phys. Rev. Lett. **101**, 077005 (2008).
- ²⁶ M.A. McGuire, A.D. Christianson, A.S. Sefat, B.C. Sales, M.D. Lumsden, R. Jin, E.A. Payzant, D. Mandrus, Y. Luan, V. Keppens, V. Varadarajan, J.W. Brill, R.P. Hermann, M.T. Sougrati, F. Grandjean, and G.J. Long, Phys. Rev. B **78**, 094517 (2008).
- ²⁷ M. Shimizu, Rep. Prog. Phys. **44**, 329 (1981).
- ²⁸ S.N. Kaul, J. Phys. Condens. Matter **11**, 7597 (1999).
- ²⁹ I.I. Mazin and D.J. Singh, Phys. Rev. B **69**, 020402(R) (2004).
- ³⁰ A. Aguayo, I.I. Mazin, and D.J. Singh, Phys. Rev. Lett. **92**, 147201 (2004).
- ³¹ S.A. Grigera, R.S. Perry, A.J. Schofield, M. Chiao, S.R. Julian, G.G. Lonzarich, S.I. Ikeda, Y. Maeno, A.J. Millis, and A.P. Mackenzie, Science **294**, 329 (2001).